

Monitoring of continuous GNSS stations in Central Anatolia region

Abdulmalek Redhwan ^{*1}, Hediye Erdoğan ¹, Osman Oktar ¹, Cemil Gezgin ¹

¹Aksaray University, Faculty of Engineering, Department of Geomatics Engineering, Aksaray, Turkey

Keywords

GNSS
ITRF
Central Anatolia Region
Time Series Analysis
Trend Component
Analysis

ABSTRACT

In this study, the linear behaviors in the North, East and Up directions of 30 CORS-TR stations in the Central Anatolian Region were obtained by the trend component analysis which is the time series component. The time series of the stations between 2017-2020 years were calculated in the Eurasia-fixed frame with the GAMIT/GLOBK software. As a result of the analysis, the average horizontal velocity of the stations in the east of the Central Anatolian Region is 17.59 mm/year in the northwest direction, and the average horizontal velocity of the stations in the west is 18.66 mm/year in the southwest direction. This movement shows the movement of the Anatolian plate in the southwest direction in terms of direction and velocity and is in agreement with other research results. In the linear changes in the up coordinates of the stations, the greatest linear change was detected at the KNY1 (-48.22 mm/year) station. It is thought that this change at station KNY1 is due to the decrease in groundwater level in this region (Konya Closed Basin). In addition, in the standard deviation (m_0) values of the time series that obtained as a result of the analysis, linear changes were approximately the same for the north and east directions, and about 2-3 times larger for the up values compared to the north or east directions.

1. INTRODUCTION

As one of the most tectonically active regions of the world, Turkey is located in an active earthquake zone. It is quite possible to encounter fault zones in engineering studies. Two of the most important (active) faults in Turkey are the North Anatolian and East Anatolian Fault Zones. The North Anatolian Fault (NAF), which extends from Karlıova in eastern Turkey to Saros Bay in the North Aegean Sea, is one of the longest active strike-slip faults in the world with a length of approximately 1500 km (Yavaşoğlu et al., 2011).

As it is known, due to the fact that Turkey is located at the intersection of the Arabian, Anatolian and Eurasian tectonic plates, annual changes (plate velocity) occur due to the movement of these plates in cm order at point locations. For this reason, it is important to determine the point location information accurately, continuously, quickly and economically with reliable methods and to present it to the relevant users who do both commercial and scientific studies in location-based studies.

Today, Global Navigation Satellite Systems (GNSS) are widely used to determine point locations. In particular, it has a wide range of uses such as tectonic movements, land subsidence, engineering services, scientific studies, aviation industry, navigation, vehicle tracking systems, military areas, and therefore has a large number of users (Uzel et al., 2013; Oktar and Erdoğan, 2018; Mutlu and Kahveci, 2019; Gezgin et al., 2020; Yalvaç, 2020; Orhan, 2021).

There are also many error sources that GNSS systems with reliable location services are exposed to. These are satellite-related such as satellite clock error, satellite orbital errors; errors originating from the receiver such as receiver clock error, antenna phase center error, and atmospheric errors such as tropospheric effect, ionospheric effect, signal reflection effect. The effect of these error sources on the results can be neglected according to the sensitivity of the work being done. However, in applications where precision is required such as geodetic studies, tectonic studies, continental deformations, it is important to create a

* Corresponding Author

*(abdulmalekredhwan2017@gmail.com) ORCID ID 0000-0003-3921-0315
(hediye.erdogan@aksaray.edu.tr) ORCID ID 0000-0002-6470-5857
(osmanoktar@aksaray.edu.tr) ORCID ID 0000-0001-6764-0561
(cemilgezgin.jfm@gmail.com) ORCID ID 0000-0002-5951-0107

Cite this article

Redhwan A., Erdoğan H., Oktar O., & Gezgin C. (2021). Monitoring of continuous GNSS stations in Central Anatolia region. Turkish Journal of Geosciences 2(2), 21-29.

mathematical model of these errors to eliminate the error sources (Mutlu and Kahveci, 2019).

In this study, the behaviors of 30 Continuously Operating Reference Stations-Turkey (TUSAGA-Aktif/CORS-TR) stations in the Central Anatolia Region were investigated with linear trend function. The coordinates of the stations were produced from the daily time series obtained between years of 2017-2020. The coordinates of the stations are the time series obtained daily between 2017 and 2020 for the Eurasia fixed-frame. The velocity values and directions of the region were estimated in the Eurasia fixed-frame by liner trend component of the time series analysis.

2. CENTRAL ANATOLIA EARTHQUAKE ZONE

Kırşehir, which is located in the great arc of Kızılırmak in Central Anatolia and consists of metamorphic and platonitic rocks, seems to have been divided into blocks from many parts by faults. The parts between the blocks were filled with Neogene sediments. These regions formed by faults are the main earthquake belts of Central Anatolia and 1938 Kırşehir earthquake occurred in this region. In this earthquake, 160 people lost their lives and 4066 buildings were destroyed or severely damaged. In addition to that 50 people died in the 1951 Kurşunlu (Çankırı) earthquake (Özdoğan, 1993).

Also, in the north of Ankara, faults in the northeast-southwest direction form parallel fracture zones in the direction of Kızılcahamam-Güdül-Ayaş and Çamlıdere-Bey pazarı. This shows that in the earthquakes in Central Anatolia, in addition to the "North Anatolian Earthquake Zone", the independent earthquake centers also have significant effects. Because the 1944 Bey pazarı and 1956 Eskişehir earthquakes are the results of an independent earthquake center. Another fault zone in Central Anatolia is located in the west of Tuz Gölü. Fractures running parallel to each other formed a belt. However, earthquakes causing massive damage were not detected either in Konya and its surroundings or in other settlements in this area (Özdoğan, 1993).

3. TIME SERIES ANALYSIS

Time series analysis provides useful information about the behavior of systems based on response or effect size. The sequential realization of the observed data over time is very important in terms of monitoring and analyzing the development of the data (Ostini, 2012).

In general, the $X(t_i)$ time series of measurements made at GNSS stations at times t_i ($i=1,2,3,\dots,N$) can be divided into three components, excluding artificial or co-seismic and seismic-induced deviations. These components are given in equation (1).

$$X(t_i) = Y(t_i)_{trend} + Y(t_i)_{periodic} + Y(t_i)_{stochastic} \quad (1)$$

In time series analysis, firstly the time axis of the series is plotted, unusual measurements (e.g. gross errors) in the series are eliminated and a general interpretation of the series can be made (Oktar, 2015).

3.1 Trend Component

Trend is the development or progress of a time series in a certain direction in the long run. The direction and intensity of the trend do not always remain constant. The trend can be linear or curvilinear (Equation 2).

$$Y(t_i) = \underbrace{a + bt}_{(1)Trend\ Component} \quad (2)$$

Here, "a" constant and "b" are the parameters that show the amount and direction of linear change with time. For GNSS stations, the increasing or decreasing linear changes (velocities) of the GNSS stations are determined with the "b" parameter. Considering the linear function given in Equation 2 for the estimation of the parameters in the time series $Y(t_i)$.

$$Y(t_i) = a + bt \quad (3)$$

$$= Ax + v(t_i) \quad (4)$$

$$A^T = \begin{bmatrix} 1 & 1 & 1, \dots, N \\ t_1 & t_2 & t_3, \dots, t_N \end{bmatrix}, X^T = [a \ b] \quad (5)$$

According to the least squares method, parameters "a", "b" and their standard deviations m_a and m_b are estimated. Test size values are calculated for each parameter.

$$t_a = \frac{a}{m_a}; t_b = \frac{b}{m_b} \quad (6)$$

The predicted $1-\alpha$ confidence level for the test sizes and the $t_{f,1-\alpha/2}$ confidence limit of the t distribution depending on the f degree of freedom are compared.

$$|t_a|; |t_b| < t_{f,1-\alpha/2} \quad (7)$$

If the situation is as seen in the equation given in 7, the parameters are insignificant,

$$|t_a|; |t_b| \geq t_{f,1-\alpha/2} \quad (8)$$

If the values above test size, parameters are significant at the estimated confidence level. If the parameters are statistically significant, it is decided that there is a trend component in the series.

In the process of determining the trend component in the time series, it is not possible to determine the existence of linear change and to accurately detect some periodic movements due to the long period of time for a full periodic movement to occur. For this reason, it is very important that the

measurements are made as long as necessary to reflect the changes in the monitored system, data or the existence of the trend must be interpreted correctly.

4. STUDY FINDINGS AND DISCUSSION

In this study, the linear behaviors of 30 TUSAGA-Aktif/CORS-TR stations in the Central Anatolia Region covering the years of 2017-2020 were investigated with the trend component function, which is the time series component. To this end; N (North), E (East) and U (Up) components of daily coordinate times series of the stations; AKD1, AKHR, AKSR, ANK2, ANRK, BEYS, BOG1, CANK, CIHA, CMLD, ESKS, GEME, GURU, HALP, KAMN, KAP1, KAYS, KIS1, KKAL, KLUU, KNY1, NAHA, NEV1, NIGD, SARV, SIH1, SIVS, SSE1, YOZ1 and YUN1 were used.

With the linear functions applied to the obtained time series, the linear changes (velocity values) of the stations in the determined time interval were calculated, and the linear behavior and functions of the stations were defined in the Eurasia Fixed system. General information about the IGS stations (14 sites) used in the processing is given in Table 1. GNSS data were evaluated with GAMIT/GLOBK software, an open-source software package developed by Massachusetts Institute of Technology (MIT) (Url-1). In the processing, for orbit information, Precise final orbits by the International Global Navigation Satellite Systems (GNSS) Service (IGS), for earth rotation parameters USNO_bull_b, for radiation and pressure effects 9-parameter Berne model was used. LC (L3), that is the ionosphere-free linear combination of the L1 and L2 carrier waves, and the FES2004 Ocean Tide Loading (OTL) grid was used. Time series of stations were obtained using

RINEX data that acquired from the web interface given in Url-2.

Table 1. IGS stations used in the processing

Station	City/ Country	Station	City / Country
ANKR	Ankara/ Turkey	MATE	Matera/ Italy
BAKU	Baku/ Azerbaijan	NICO	Nicosia/ South Cyprus
BUCU	Bucharest/ Romania	RAMO	MitzpeRamon/ Israel
CRAO	Simeiz/ Ukraine	SOFI	Sofia/ Bulgaria
GLSV	Kiev/ Ukraine	TEHN	Tehran/ Iran
GRAZ	Graz/Austria	TELA	Tel Aviv/ Israel
ISTA	İstanbul/ Turkey	TUBI	Gebze/ Turkey

4.1 The Field Study and Data

In this study, daily coordinate data of the 30 GNSS stations such as AKD1, AKHR, AKSR, ANK2, ANRK, BEYS, BOG1, CANK, CIHA, CMLD, ESKS, GEME, GURU, HALP, KAMN, KAP1, KAYS, KIS1, KKAL, KLUU, KNY1, NAHA, NEV1, NIGD, SARV, SIH1, SIVS, SSE1, YOZ1 and YUN1 were used in the analysis that located in the Central Anatolia Region. Location information of the stations are given in Figure 1 and Table 2. The GNSS data used in the study are the daily coordinate values between 01.01.2017 and 31.12.2020, and the data information of the stations are given in Table 3. In the evaluations and analyzes, there were data deficiencies and gaps between years in the daily coordinate data of GNSS stations between 01.01.2017-31.12.2020 due to reasons such as antenna defect, computer malfunction, etc.

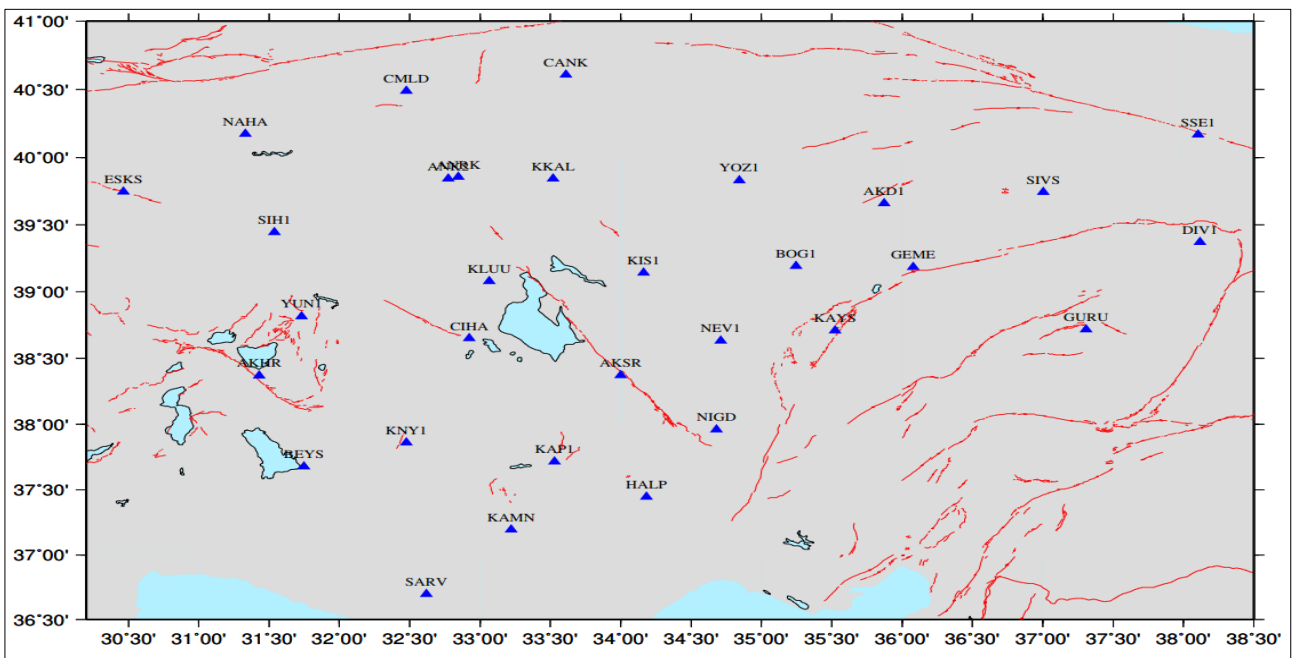


Figure 1. GNSS stations locations

Table 2. GNSS stations general information

Short Name	City/ Town	Latitude (Decimal Degree)	Longitude (Decimal Degree)	Short Name	City/ Town	Latitude (Decimal Degree)	Longitude (Decimal Degree)
AKD1	Yozgat/Akdağmadeni	39.6605	35.8711	KAP1	Konya/Karapınar	37.7144	33.5283
AKHR	Konya/Akşehir	38.3693	31.4297	KAYS	Kayseri/Melikgazi	38.7137	35.5031
AKSR	Aksaray/Merkez	38.3704	33.9982	KIS1	Kırşehir/Merkez	39.1434	34.1631
ANK2	Ankara/Çankaya	39.8428	32.7754	KKAL	Kırıkkale/Merkez	39.8433	33.5179
ANRK	Ankara/Çankaya	39.8560	32.8462	KLUU	Konya/Kulu	39.0791	33.0654
BEYS	Konya/Beyşehir	37.6773	31.7466	KNY1	Konya/Meram	37.8594	32.4764
BOG1	Yozgat/Boğazlıyan	39.1933	35.2471	NAHA	Ankara/Nallıhan	40.1733	31.3321
CANK	Çankırı/Merkez	40.6086	33.6104	NEV1	Nevşehir/Merkez	38.6315	34.7108
CIHA	Konya/Cihanbeyli	38.6504	32.9224	NIGD	Niğde/Merkez	37.9588	34.6794
CMLD	Ankara/Çamlidere	40.4910	32.4745	SARV	Karaman/Sarveliler	36.6967	32.6173
DIV1	Sivas/Divriği	39.3718	38.1194	SIH1	Eskişehir/Sivrihisar	39.4465	31.5363
ESKS	Eskişehir/Turgutlar	39.7457	30.4636	SIVS	Sivas/Merkez	39.7437	37.0025
GEME	Sivas/Gemerek	39.1851	36.0809	SSE1	Sivas/Suşehri	40.1691	38.1050
GURU	Sivas/Gürün	38.7174	37.3079	YOZ1	Yozgat/Merkez	39.8314	34.8447
HALP	Konya/Halkapınar	37.4451	34.1834	YUN1	Konya/Yunak	38.8162	31.7317
KAMN	Karaman/Merkez	37.1932	33.2203				

Data numbers and missing data percentages of these stations are given in Table 3. Data percentages of other stations are certain except AKD1, ANRK, BOG1, CANK, CMLD, KAP1, KAYS, KIS1, SARV, SIH1,

SIVS, YOZ1 and YUN1. In addition, since KIS1 and ANK2 stations are newly established, their data is used for 1 year, AKD1 station for 2 years, BOG1, NEV1 and SSE1 for 3 years.

Table 3. GNSS stations data and percentages

Station Name	Beginning	Finish	Number of Data	Missing Data(%)	Station Name	Beginning	Finish	Number of Data	Missing Data(%)
AKD1	01.01.2019	31.12.2020	620	0.8	KAP1	19.06.2017	31.12.2020	1268	0.9
AKHR	01.01.2017	31.12.2020	1460	0	KAYS	01.01.2017	31.12.2020	1436	1
AKSR	01.01.2017	31.12.2020	1455	0	KIS1	12.02.2020	31.12.2020	323	0.9
ANK2	01.01.2020	31.12.2020	365	0	KKAL	01.01.2017	31.12.2020	1460	0
ANRK	01.01.2017	31.12.2020	1435	1	KLUU	01.01.2017	31.12.2020	1460	0
BEYS	01.01.2017	31.12.2020	1460	0	KNY1	01.01.2017	31.12.2020	1460	0
BOG1	01.01.2018	31.12.2020	1095	0.7	NAHA	01.01.2017	31.12.2020	1460	0
CANK	01.01.2017	31.12.2020	1431	0.9	NEV1	01.01.2018	31.12.2020	1095	0
CIHA	01.01.2017	31.12.2020	1460	0	NIGD	01.01.2017	31.12.2020	1460	0
CMLD	01.01.2017	31.12.2020	1411	1	SARV	01.01.2017	31.12.2020	1263	0.9
ESKS	01.01.2017	31.12.2020	1460	0	SIH1	01.01.2017	25.06.2020	1047	0.7
GEME	01.01.2017	31.12.2020	1460	0	SIVS	01.01.2017	31.12.2020	1169	0.8
GURU	01.01.2017	31.12.2020	1460	0	SSE1	01.01.2018	31.12.2020	1095	0
HALP	01.01.2017	31.12.2020	1460	0	YOZ1	01.01.2017	31.12.2020	1405	1
KAMN	01.01.2017	31.12.2020	1460	0	YUN1	01.01.2017	31.12.2020	1397	1

4.2 GNSS Stations Time Series

For the time series analysis, BASK, SIVS, YAZ1, CANK, ANRK, CALM, AKD1 and YUN1 stations were considered as two data groups, and SARV and SIH1 stations as three data groups due to the large data gaps in some of the stations. The time interval of time series data obtained by taking Eurasia plate as constant is given in Table 3.

In this study, raw coordinate time series were created by subtracting the first coordinate value

from all coordinates in order to see the change of raw coordinates relative to the beginning.

In Figure 2, 3 and 4, it is clearly seen that the time series of KAP1 North (increase), East (decrease) and Up (decrease) raw coordinates contain a linear movement, and in addition, a one (1) year periodic movement is seen in the time series of the northing coordinates. Time series of the remaining stations are not given in this study due to the large number of data and figures.

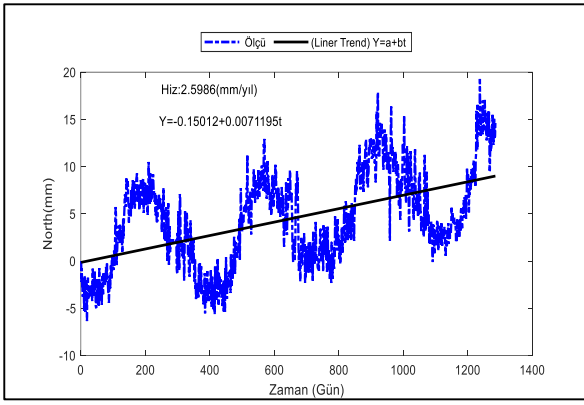


Figure 2. KAP1 North coordinate component linear model

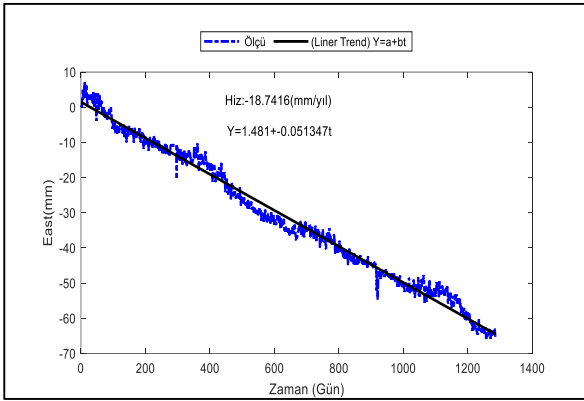


Figure 3. KAP1 East coordinate component linear model

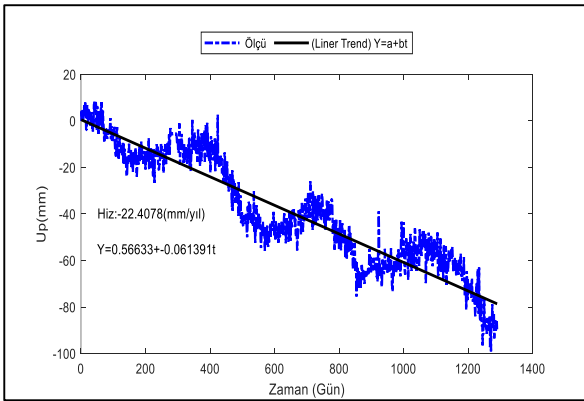


Figure 4. KAP1 Up coordinate component linear model

The linear trend component analysis of the time series was performed by calculating the “a” and “b” parameters and standard deviations given in Equation 3.2 according to the least squares method. The calculated test sizes were compared with the $\alpha=0.05$ significance level and the $t_{f,1-\alpha/2}$ confidence limit of the t distribution depending on the f degree of freedom, and statistically significant linear

movements were detected in the time series of all GNSS stations. Obtained results and functions are given in Table 4.

When Table 4 is examined, it is seen that CANK_1, CIHA, ANRK_1, ANKR, SERV_2, CALM_1, CALM_2, BEYS, YUN1_1, YUN1_2, SIH1_1, SIH1_2, SIH1_3, AKHR, NAHA, ESKS, BUCU and ANK2 stations have linear movements in the south direction, while the other stations have linear movements in the north direction.

The eastward movements were detected in stations; BASK_1, BASK_2, GURU, SIVS_1, SIVS_2, GEME, KAYS, YOZ1_1, YOZ1_2, NIGD, HALP, AKSR, CANK_1, CANK_2, KKAL, KAMN, KLUU, CIHA, ANRK_1, ANRK_2, ANKR, SARV1, SARV_2, SARV_3, CALM_1, CALM_2, BEYS, YUN1_1, YUN_2, SIH1_1, SIH1_2, AKHR, NAHA, ESKS, BOR1, KAP1, BOG1, NIV1, AKD1_1, AKD1_2, ANK2, KIS1 and westward movements were detected at SIH1_3 and BUCU stations. The largest linear movement in the west direction (23.29 mm/year) was detected at ANKR station, and the smallest linear movement (0.36 mm/year) was detected at BUCU station.

In addition, the largest annual linear movement in the north direction of 15.51 mm was observed at BASK_1 station, and the smallest annual linear movement in the south direction of 0.06 mm was observed at ANRK_1 station. Considering the linear movements in the time series of the Up coordinates of the stations; (Table 4) BASK_1, BASK_2, SIVS_1, SIVS_2, GEME, KAYS, YOZ1_1, YOZ1_2, NIGD, HALP, KKAL, KLUU, ANRK_1, ANRK_2, SARV_2, SARV_3, CALM_1, CALM_2, BEYS, YUN1_1, YUNH1_2, KSSI, BUCU, SSE1, AKD1_2 and ANK2 linear movements in the direction were observed in the positive direction, it was seen that the up values of the stations listed above are increased.

The highest linear motion was calculated at the SARV_3 station with a value of 29.75 mm/year and the lowest linear motion was calculated at the YOZ1_2 station with a value of 0.10 mm/year. Linear movements in up coordinates of GURU, AKSR, CANK_1, CANK_2, KAMN, CIHA, ANKR, SARV_1, KNY1, SIH1_3, AKHR, KAP1, BOG1, NIV1, and AKD1_1 stations are in (-) negative direction. In the up time series, the largest linear movement was detected at KNY1 station with a value of -48.22 mm/year and the smallest linear movement was determined at station NEV1 with a value of -0.15 mm/year. In addition, a change of approximately -22.41 mm/year is observed at KAP1 station (Table 4). It is thought that the KNY1 and KAP1 stations are located in the areas where the groundwater level decreases in the Konya Closed Basin, and the negative (-) change in these stations is related with the decrease in the water level. Many studies have been carried out on the decrease in groundwater level in this region. See for detailed information; Üstün et al. 2007; Üstün et al. 2015; Özdemir, 2014; Orhan et al. 2020; Orhan 2021.

Table 4. Linear models and annual rates of GNSS stations (Eurasian-fixed frame)

Station Name	$y(t) = a+bt$ NORTH Linear Model	Speed = $365*b$ (mm/year)	$y(t) = a+bt$ EAST Linear Model	Speed = $365*b$ (mm/year)	Resultant Speed (mm/year)		$y(t) = a+bt$ Up Linear Model	Speed = $365*b$ (mm/year)
BASK_1	$y(t) = 1.341+0.0425t$	15.51	$y(t) = -2.5443-0.0133t$	-4.84	16.25	Northwest	$y(t) = -5.1855+0.0193t$	7.04
BASK_2	$y(t) = 0.0217+0.0419t$	15.29	$y(t) = -1.7058-0.0126t$	-4.61	15.97	Northwest	$y(t) = 8.6337+0.0138t$	5.02
GURU	$y(t) = 0.7210+0.0252t$	9.19	$y(t) = -0.1948-0.0438t$	-15.99	18.44	Northwest	$y(t) = 1.6579-0.0006t$	-0.22
SIVS_1	$y(t) = 0.3337+0.0194t$	7.08	$y(t) = -0.3377-0.0439t$	-16.01	17.50	Northwest	$y(t) = -3.1008+0.0163t$	5.97
SIVS_2	$y(t) = -2.1542+0.0236t$	8.63	$y(t) = -4.4541-0.0497t$	-18.13	20.08	Northwest	$y(t) = -21.3763+0.0042t$	1.52
GEME	$y(t) = -7.7208+0.0247t$	9.01	$y(t) = -2.3107-0.0418t$	-15.25	17.71	Northwest	$y(t) = -0.9210+0.0033t$	1.22
KAYS	$y(t) = -0.1221+0.0181t$	6.61	$y(t) = 0.0131-0.0442t$	-16.14	17.44	Northwest	$y(t) = 3.6273+0.0003t$	0.11
YOZ1_1	$y(t) = 0.8331+0.0103t$	3.75	$y(t) = 3.2804-0.0480t$	-17.53	17.92	Northwest	$y(t) = -5.2383+0.0119t$	4.35
YOZ1_2	$y(t) = 3.2809+0.0130t$	4.76	$y(t) = -0.3345-0.0511t$	-18.64	19.24	Northwest	$y(t) = -6.5517+0.0003t$	0.10
NIGD	$y(t) = -0.0879+0.0146t$	5.31	$y(t) = -1.6882-0.0408t$	-14.89	15.81	Northwest	$y(t) = -23.8459+0.0016t$	0.59
HALP	$y(t) = 1.1983+0.0151t$	5.53	$y(t) = -0.8474-0.0387t$	-13.41	14.50	Northwest	$y(t) = -6.7455+0.0028t$	1.04
AKSR	$y(t) = -1.3001+0.0085t$	3.10	$y(t) = 2.8935-0.0516t$	-18.82	19.07	Northwest	$y(t) = -14.5906-0.0205t$	-7.48
CANK_1	$y(t) = 1.9777-0.0017t$	-0.63	$y(t) = -2.5724-0.0482t$	-17.59	17.60	Southwest	$y(t) = -0.8255-0.0009t$	-0.33
CANK_2	$y(t) = -1.8853+0.0180t$	6.56	$y(t) = -1.0364-0.0439t$	-16.01	17.31	Northwest	$y(t) = 5.6662-0.0141t$	-5.15
KKAL	$y(t) = -0.4284+0.0038t$	1.39	$y(t) = 1.5088-0.0578t$	-21.11	21.16	Northwest	$y(t) = -12.8039+0.0030t$	1.08
KAMN	$y(t) = -1.4761+0.0119t$	4.36	$y(t) = 0.1776-0.0336t$	-12.28	13.03	Northwest	$y(t) = -19.9852-0.0137t$	-5.00
KLUU	$y(t) = -1.1815+0.0074t$	2.70	$y(t) = -1.3936-0.0522t$	-19.04	19.23	Northwest	$y(t) = -0.5096+0.0032t$	1.19
CIHA	$y(t) = 0.9653-0.0012t$	-0.45	$y(t) = 1.4483-0.0563t$	-20.55	20.55	Southwest	$y(t) = 1.0117-0.0079t$	-2.89
ANRK_1	$y(t) = 2.0997-0.0002t$	-0.06	$y(t) = 0.4200-0.0621t$	-22.66	22.66	Southwest	$y(t) = -5.7743+0.0111t$	4.06
ANRK_2	$y(t) = -0.7142+0.0006t$	0.23	$y(t) = 0.5205-0.0565t$	-20.64	20.64	Northwest	$y(t) = -4.8296+0.0135t$	4.93
ANKR	$y(t) = -0.1372-0.0023t$	-0.82	$y(t) = -2.1792-0.0638t$	-23.29	23.31	Southwest	$y(t) = -13.43-0.0124t$	-4.54
SARV_1	$y(t) = 1.8299+0.0077t$	2.81	$y(t) = -1.4094-0.0421t$	-15.36	15.61	Northwest	$y(t) = -12.3092-0.0047t$	-1.72
SARV_2	$y(t) = 4.1808-0.0233t$	-8.49	$y(t) = -6.1333-0.0213t$	-7.76	11.50	Southwest	$y(t) = -12.0975+0.0706t$	25.76
SARV_3	$y(t) = 4.5048+0.0149t$	5.45	$y(t) = -0.2086-0.0600t$	-21.90	22.57	Northwest	$y(t) = 7.528+0.0815t$	29.75
KNY1	$y(t) = 5.7047+0.0217t$	7.93	$y(t) = -5.6043-0.0505t$	-18.42	20.06	Northwest	$y(t) = -42.4959-0.1321t$	-48.22
CALM_1	$y(t) = 1.6803-0.0046t$	-1.66	$y(t) = 1.4626-0.0540t$	-19.71	19.78	Southwest	$y(t) = -3.4678+0.0065t$	2.38
CALM_2	$y(t) = 0.5128-0.0043t$	-1.58	$y(t) = 1.3307-0.0524t$	-19.14	19.21	Southwest	$y(t) = -4.3832+0.0011t$	0.39
BEYS	$y(t) = 0.4754-0.0076t$	-2.77	$y(t) = -0.4252-0.0436t$	-15.92	16.15	Southwest	$y(t) = -9.6745+0.0047t$	1.70
YUN1_1	$y(t) = -0.7425-0.0068t$	-2.48	$y(t) = 1.006-0.0575t$	-20.99	21.13	Southwest	$y(t) = 0.1629+0.0139t$	5.08
YUN1_2	$y(t) = -0.3143-0.0084t$	-3.07	$y(t) = 5.7488-0.0545t$	-19.89	20.13	Southwest	$y(t) = 3.9402+0.0155t$	5.65
SIH1_1	$y(t) = -0.9776-0.0085t$	-3.10	$y(t) = 0.1050-0.0603t$	-22.01	22.23	Southwest	$y(t) = 1.5454+0.0105t$	3.83
SIH1_2	$y(t) = 0.6935-0.0193t$	-7.06	$y(t) = 0.6006-0.0602t$	-21.98	23.08	Southwest	$y(t) = -2.7725+0.0125t$	4.57
SIH1_3	$y(t) = 2.1295-0.0230t$	-8.40	$y(t) = 1.6909-0.0569t$	0.81	8.44	Southeast	$y(t) = -1.4834-0.0171t$	-6.26
AKHR	$y(t) = 12.1708-0.0121t$	-4.42	$y(t) = -5.1438-0.0575t$	-20.97	21.43	Southwest	$y(t) = 4.2996-0.0096t$	-3.49
NAHA	$y(t) = 2.3182-0.0069t$	-2.52	$y(t) = -0.3622-0.0592t$	-21.61	21.76	Southwest	$y(t) = -1.085+0.0068t$	2.50
ESKS	$y(t) = 0.0218-0.0090t$	-3.28	$y(t) = 2.7517-0.0586t$	-21.23	21.48	Southwest	$y(t) = -2.5633+0.0053t$	1.85
BUCU	$y(t) = -0.1475-0.0030t$	-1.11	$y(t) = -0.3426+0.0010t$	0.36	1.17	Southeast	$y(t) = -1.6873+0.0059t$	2.17
KAP1	$y(t) = -0.1501+0.0071t$	2.60	$y(t) = 1.481-0.0513t$	-18.74	18.92	Northwest	$y(t) = 0.5663-0.0614t$	-22.41
SSE1	$y(t) = 0.6549+0.0164t$	5.98	$y(t) = 0.3114-0.0289t$	-10.54	12.12	Northwest	$y(t) = -2.0701+0.0046t$	1.67
BOG1	$y(t) = -1.6183+0.0161t$	5.88	$y(t) = 4.8055-0.0530t$	-19.34	20.21	Northwest	$y(t) = -6.6115-0.0096t$	-3.51
NIV1	$y(t) = 2.7078+0.0187t$	6.84	$y(t) = 2.2719-0.0471t$	-17.21	18.52	Northwest	$y(t) = 2.5191-0.0004t$	-0.15
AKD1_1	$y(t) = -3.6114+0.0371t$	13.53	$y(t) = -4.554-0.0439t$	-16.01	20.96	Northwest	$y(t) = -21.0493-0.0254t$	-9.28
AKD1_2	$y(t) = 3.1354+0.0192t$	7.01	$y(t) = 9.3971-0.0552t$	-20.16	21.35	Northwest	$y(t) = -2.2247+0.0043t$	1.56
ANK2	$y(t) = 2.1425-0.0012t$	-0.44	$y(t) = 0.5857-0.0664t$	-24.25	24.26	Southwest	$y(t) = -0.8576+0.0148t$	5.41
KIS1	$y(t) = -2.1063+0.0155t$	5.64	$y(t) = -1.9041-0.0548t$	-20.01	20.79	Northwest	$y(t) = 3.4692+0.0183t$	6.69

In Table 4, the average horizontal movement (resultant velocity) was found to be 18.24 mm/year in the northwest direction and 18.66 mm/year in the southwest direction. When the results obtained for

the horizontal component from this study compared with other studies that given in Figure 5, such as, the velocity value of 20 mm/year in the southwest direction obtained from Cingöz et al. (2013), and

value of 21.72 mm/year obtained by Güllal et al. 2013 and the velocity of 20.52 mm/year by Güçlü 2021, around Kırıkkale, it is seen that the velocity values obtained from this study is in agreement with these studies.

In addition, it has been shown that the Anatolian Plate has a westward linear movement with a velocity of 13-27 mm/year (Şentürk, 2019) and the North Anatolian Fault Zone has a westward movement of approximately 25 mm/year relative to the Eurasian Plate (Aktuğ, 2006). In the study conducted by Tiryakioğlu (2012), it was determined that the velocities parallel to the fault was approximately 22 mm/year at the points in Southwest Anatolia and the north of the Fethiye-Burdur Fault Zone.

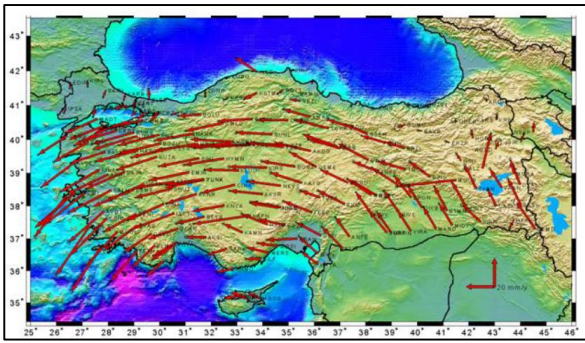


Figure 5. Point velocities (Eurasia fixed) (Cingöz et al., 2013)

It has also been determined that the results obtained from this study in the vertical component are in agreement with the vertical velocity values given in Figure 6.

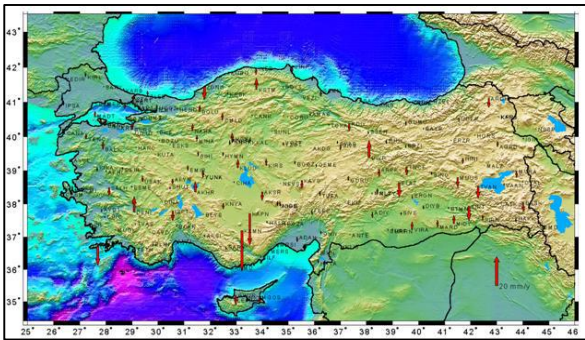


Figure 6. Point velocities (vertical) (Özdemir et al., 2011)

Additionally, the standard deviation values (m_0) of the linear changes in the time series were also calculated. The m_0 values calculated for each station as a result of the adjustment in the north, east and Up directions, are given in Figure 7, 8 and 9. As it is seen (Figure 7, 8, 9), for the north direction of the stations, the m_0 values are in the range of approximately 1-4 mm, excluding SARV_1 ($m_0=4.89\text{mm}$), and KAP1 ($m_0=4.25\text{mm}$) stations, for the east direction, SARV_3 ($m_0=4.72\text{ mm}$) station. It is seen that the m_0

values are in the range of 0.8-3.5 mm except for the up direction, the biggest standard deviation is KNY1 ($m_0=18.01\text{ mm}$) station and the other stations m_0 values are in the range of 3-13 mm. Due to the insufficient number of data (data gap), the m_0 values of the SARV station, which were examined in three parts, were found to be higher than the other stations.

While the obtained m_0 values are approximately same for the north and east directions, it can be stated that the Up values are approximately 2-3 times greater than the north or east directions. As it is known, the fact that the sensitivity of the up component determined by GNSS is 2-3 times worse than the horizontal position sensitivity is also seen in the results obtained here.

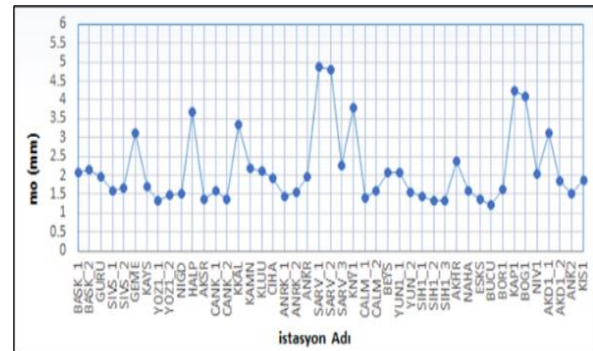


Figure 7. North direction linear variations standard deviations (m_0)

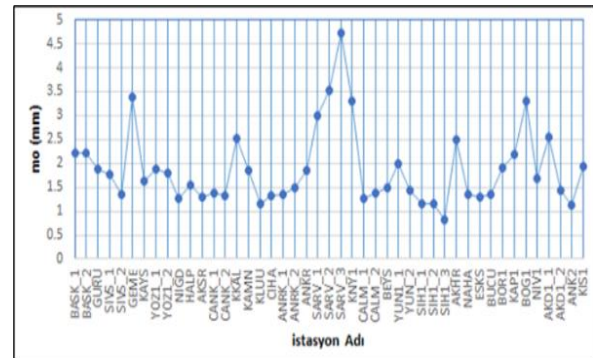


Figure 8. East direction linear variations standard deviations (m_0)

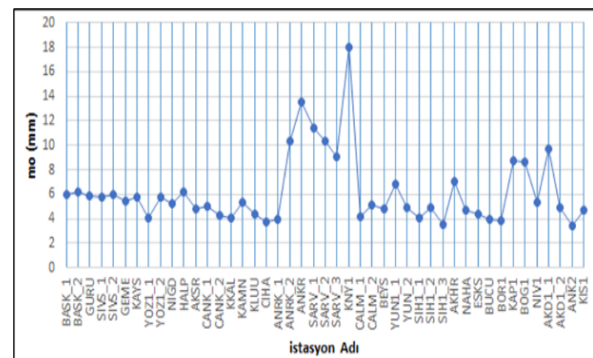


Figure 9. Up direction linear variations standard deviations (m_0)

5. RESULTS

Since Turkey is located at the intersection of Arabian, Anatolian and Eurasian tectonic plates, annual changes occur in point positions at the rank of cm due to the movement of these plates. For this reason, obtaining, evaluating, analyzing (time series analysis) and calculating the velocity values of GNSS stations at certain time intervals (daily, monthly, etc.) are important in terms of determining the position accuracy of the GNSS sites and ensuring their continuity.

In this study; The linear behaviors in the North, East and Up directions of 30 CORS-TR GNSS stations located in the Central Anatolian Region were obtained with the trend component analysis, which is the time series analysis component. The time series of the stations between the years of 2017 - 2020 were calculated with the GAMIT/GLOBK software, taking Eurasia plate as constant.

In the result of the analysis, it is obtained that the BASK_1, BASK_2, GURU, SIVS_1, SIVS_2, GEME, KAYS, YOZ1_1, YOZ1_2, NIGD, HALP, AKSR, CANK_2, KKAL, KAMN, KLUU, ANRK_2, SARV_1, SARV_3, KNY1, KAP1, SSE1, BOG1, NIV1, AKD1_1, AKD1_2 and KIS1 stations have an average horizontal velocity of 17.59 mm/year in the northwest direction and CANK_1, CIHA, ANRK_1, ANKR, SARV_2, CALM_1, CALM_2, BEYS, YUN1_1, YUN_2, SIH1_1, SIH1_2, AKHRSI, ESKS, BUCU and ANK2 stations have an average horizontal velocity of 18.66 mm/year in the southwest direction. This shows the movement of the Anatolian plate in the southwest direction in terms of movement direction and velocity value and is consistent with other research results.

In the linear changes in the Up coordinates of the stations, the largest linear movement in the (+) positive direction was determined at the SARV_3 station with 29.75 mm/year values, and the largest linear movement in the negative (-) direction was determined at the KNY1 station with the values of -48.22 mm/year. Also, 22.41 mm/year change was observed in the Up coordinate in negative direction at the KAP1 station. It is thought that the negative (-) change in these station is occurred due to the decrease in the groundwater level in this region (Konya Closed Basin).

In addition, standard deviation values (m_0) were calculated as a result of the analysis of the linear changes of time series, and due to the high number of data loss, the m_0 values of the SARV station, which were examined in three separate parts, were found to be large than the other stations. While the obtained m_0 values are approximately the same for the north and east directions, it can be stated that the Up values are approximately 2-3 times larger than the north or east directions. As it is known, the sensitivity of the Up values determined by GNSS is 2-3 times worse than the horizontal position sensitivity, is also seen in the results obtained from this study.

Acknowledgement

This article was produced from Abdulmalek REDHWAN's master thesis.

Author Contributions

Abdulmalek Redhwan: Methodology, Software, Validation, Formal analysis, Writing-Original Draft, Visualization. **Hediye Erdoğan:** Supervision, Writing-Original Draft. **Osman Otkar:** Methodology, Software, Formal analysis. **Cemil Gezgin:** Writing-Review & Editing, Visualization.

Conflicts of Interest

The authors declare no conflict of interest

REFERENCES

- Aktuğ, B. (2006). Determination of earthquake source parameters through geodetic observations (PhD thesis). Istanbul Technical University, Istanbul, Turkey (in Turkish).
- Cingöz, A., Erkan, Y., Kurt, Y.A., & Peker, S. (2013). Turkey national fixed gnss network-active (TUSAGA-Active) system. *TMMOB Chamber of Surveying and Cadastre Engineers, 14. Turkey Map Scientific and Technical Congress*, Ankara.
- Gezgin, C., Tiryakioğlu, İ., Ekercin, S., & Gürbüz, E. (2020). Monitoring of tectonic movements of the southern section of the Tuz Gölü fault zone (TGFZ) with GNSS observations. *Afyon Kocatepe University Journal of Science and Engineering*, 20(3), 456-464.
- Güçlü, A.T. (2021). Definition of behavior of GNSS stations in Kırıkkale and surrounding (MSc thesis). Aksaray University, Aksaray, Turkey (in Turkish).
- Gülal, E., Aykut, N.O., Akpınar, B., Tiryakioğlu, İ., Dindar, A.A., & Erdoğan, H. (2013). Establishment of Yildiz Technical University fixed GNSS station, analysis and presentation of data, 14. *Turkey Map Scientific Technical Congress*, Ankara.
- Mutlu, İ., & Kahveci, M. (2019). The importance of GNSS satellite distribution in Real-Time Kinematics GNSS and Network-RTK measurements. *Geomatics*, 4(3), 179-189.
- Otkar, O. (2015). Identification of behavior of stationary GNSS stations with wavelet transform (MSc thesis). Aksaray University, Aksaray, Turkey (in Turkish).
- Otkar, O., & Erdogan, H. (2018). Research of behaviours of continuous GNSS stations by

- signal. *Earth Sciences Research Journal*, 22(1), 19-27.
- Orhan, O., Yakar, M., & Ekercin, S. (2020). An application on sinkhole susceptibility mapping by integrating remote sensing and geographic information systems. *Arabian Journal of Geosciences*, 13,17, 1-17.
- Orhan, O. (2021). Monitoring of land subsidence due to excessive groundwater extraction using small baseline subset technique in Konya, Turkey. *Environmental Monitoring and Assessment*, 193(4), 1-17.
- Orhan, O., Oliver-Cabrera, T., Wdowski, S., Yalvac, S., & Yakar, M. (2021). Land subsidence and its relations with sinkhole activity in Karapınar region, Turkey: a multi-sensor InSAR time series study. *Sensors*, 21(3), 774.
- Ostini, L. (2012). Analysis and quality assessment of GNSS-derived parameter time series (PhD thesis). Bern University, Bern, Switzerland.
- Özdemir, S. (2014). Analysis of GNSS time series obtained from Turkish national permanent GNSS stations network-active system using Hilbert-Huang transform (MSc thesis). Middle East Technical University, Ankara Turkey.
- Özdemir, S., Cingöz, A., Aktuğ, B., Lenk, O., Kurt, M., & Parmaksız, E. (2011). Analysis of fixed station data. *TMMOB Chamber of Surveying and Cadastre Engineers 13th Turkish Scientific and Technical Mapping Congress*, 18-22.
- Özdoğan, S. (1993). Turkey's earthquake zones. *Journal of Turkish Geography Research and Application Center*, 2, 53-68.
- Şentürk, M.D. (2019). Optimal filtering of strong motion records with GPS (MSc thesis). Ankara University, Ankara, Turkey (in Turkish).
- Tiryakioğlu, İ. (2012). identification of the block movements and stress zones in southwestern anatolia with GNSS measurements (PhD thesis). Yıldız Technical University, İstanbul, Turkey (in Turkish).
- Uzel, T., Eren, K., Gulal, E., Tiryakioğlu, I., Dindar, A. A., & Yılmaz, H. (2013). Monitoring the tectonic plate movements in Turkey based on the national continuous GNSS network. *Arabian Journal of Geosciences*, 6(9), 3573-3580.
- Üstün, A., Tuşat, E., & Abbak, R.A. (2007). Groundwater withdrawal in Konya Closed Basin and geodetic monitoring of possible consequences. *3. Engineering Symposium*, 24-26.
- Üstün, A., Tuşat, E., Yalvaç, S., Özkan, İ., Eren, Y., Özdemir, A., & Doğanalp, S. (2015). Land subsidence in Konya Closed Basin and its spatio-temporal detection by GPS and DInSAR. *Environmental earth sciences*, 73,10, 6691-6703.
- Yalvaç, S. (2020). Determining the effects of the 2020 Elazığ-Sivrice/Turkey (Mw 6.7) earthquake from the surrounding CORS-TR GNSS stations. *Turkish Journal of Geosciences*, 1(1), 15-21.
- Yavaşoğlu, H., Tarı, E., Tüysüz, O., Çakır, Z., & Ergintav, S. (2011). Determining and modeling tectonic movements along the central part of the North Anatolian Fault (Turkey) using geodetic measurements. *Journal of Geodynamics*, 51,5, 339-343.
- Url-1: http://geoweb.mit.edu/gg/GAMIT_Ref.pdf, (last accessed 10 July 2020)
- Url-2: <http://tusaga.aktif.gov.tr/Sayfalar/Rinex/30snRinex.aspx>, (last accessed 4 July 2020)



© Author(s) 2021. This work is distributed under <https://creativecommons.org/licenses/by-sa/4.0/>